The mitochondrial monothiol glutaredoxin S15 is essential for iron-sulfur protein maturation in *Arabidopsis thaliana*

Anna Moseler[a], Isabel Aller[a], Stephan Wagner[b], Thomas Nietzel[b], Jonathan Przybyla-Toscano[c,d], Ulrich Mühlenhoff[e], Roland Lill[e], Carsten Berndt[f], Nicolas Rouhier[c,d,e], Markus Schwarzländer[b], and Andreas J. Meyer[a,g,1]

[a]Institute of Crop Science and Resource Conservation (INRES)-Chemical Signalling, University of Bonn, 53113 Bonn, Germany; [b]INRES-Plant Energy Biology, University of Bonn, 53113 Bonn, Germany; [c]Unité Mixte de Recherche (UMR) 1136 Interactions Arbres/Microorganismes, Faculté des Sciences et Technologies, Université de Lorraine, 54506 Vandoeuvre-lès-Nancy, France; [d]UMR 1136 Interactions Arbres/Microorganismes, Centre Institut National de la Recherche Agronomique (INRA) Nancy Lorraine, INRA, 54280 Champenoux, France; [e]Institut für Zytobiologie, Philipps-Universität Marburg, 35032 Marburg, Germany; [f]Department of Neurology, Medical Faculty, Heinrich-Heine-University Düsseldorf, 40225 Düsseldorf, Germany; and [g]Bioeconomy Science Center, c/o Forschungszentrum Jülich, 52425 Jülich, Germany

Edited by Bob B. Buchanan, University of California, Berkeley, CA, and approved September 15, 2015 (received for review June 2, 2015)

The iron-sulfur cluster (ISC) is an ancient and essential cofactor of many proteins involved in electron transfer and metabolic reactions. In *Arabidopsis*, three pathways exist for the maturation of iron-sulfur proteins in the cytosol, plastids, and mitochondria. We functionally characterized the role of mitochondrial glutaredoxin S15 (GRXS15) in biogenesis of ISC containing aconitase through a combination of genetic, physiological, and biochemical approaches. Two *Arabidopsis* T-DNA insertion mutants were identified as null mutants with early embryonic lethal phenotypes that could be rescued by GRXS15. Furthermore, we showed that recombinant GRXS15 is able to coordinate and transfer an ISC and that this coordination depends on reduced glutathione (GSH). We found the *Arabidopsis* GRXS15 able to complement growth defects based on disturbed ISC protein assembly of a yeast Δ*grx5* mutant. Modeling of GRXS15 onto the crystal structures of related nonplant proteins highlighted amino acid residues that after mutation diminished GSH and subsequently ISC coordination, as well as the ability to rescue the yeast mutant. When used for plant complementation, one of these mutant variants, $GRXS15_{K83/A}$, led to severe developmental delay and a pronounced decrease in aconitase activity by approximately 65%. These results indicate that mitochondrial GRXS15 is an essential protein in *Arabidopsis*, required for full activity of iron-sulfur proteins.

glutaredoxin | iron-sulfur cluster | mitochondria | aconitase | glutathione

Iron-sulfur cluster (ISC) containing proteins conduct essential metabolic processes in all organisms. In plants, autonomous pathways for ISC assembly are present in plastids and mitochondria, whereas ISC biosynthesis and incorporation in cytosolic and nuclear proteins relies on export of bound sulfide from mitochondria (1). Because ISCs are sensitive to superoxide and its reaction products formed by aerobic metabolism, increasing oxidation of the atmosphere led to evolution of sophisticated machineries mediating and controlling the assembly and the transfer of ISCs to acceptor proteins (2). The entire machinery consisting of more than 14 proteins in plastids and 19 proteins in mitochondria includes proteins providing sulfur and iron atoms, scaffold proteins for cluster assembly and transfer proteins that insert ISCs into recipient apoproteins (3). The fundamental role of ISC assembly for building the machineries that are at the center of maintaining life is emphasized by the fact that mutants affecting genes of the ISC assembly pathways are frequently embryo-lethal (3). Among the proteins considered as transfer proteins are representatives of the type II subset of glutaredoxins (GRX), which are characterized by their CGFS monothiol active site motif and their ability to bind glutathione-bridged ISCs (4).

Although evidence exists for the function of GRXs in the assembly of Fe-S proteins in yeast cells and vertebrates (5, 6), their significance in planta is still unclear. Null mutants for plastidic monothiol GRXS14 and GRXS16 are viable, which may be explained by partially overlapping activities (3). Nevertheless, the ability of both proteins to complement the yeast Δ*grx5* mutant that lacks the mitochondrial monothiol Grx5p strongly hints to involvement in maturation of Fe-S proteins (7). Similarly, it has been shown that the cytosolic and nuclear GRXS17, both from poplar and *Arabidopsis*, can also complement the Δ*grx5* mutant (7, 8). However, *Arabidopsis grxs17* null mutants had only a minor decrease in cytosolic Fe-S enzyme activities, whereas a severe developmental phenotype is visible under elevated temperature and extended daylight. These data indicate that GRXS17 is likely not required for de novo ISC assembly in the cytosol, although it could play a role in cluster repair. Rather, it may be that GRXS17 functions as an oxidoreductase, regulating the function of its partners as BolA2, NF-YC11, or other unidentified targets (8, 9).

However, the involvement of GRXS15 in the maturation of Fe-S proteins in mitochondria remains elusive in plants because, among poplar monothiol GRXs, it is the only isoform failing to rescue most phenotypes of the yeast Δ*grx5* mutant (7). Furthermore, the subcellular localization of GRXS15 is ambiguous. Independent targeting experiments have reported GFP-tagged poplar GRXS15 in

Significance

Monothiol glutaredoxins have been considered as components of the iron-sulfur protein assembly machinery but lack of suitable mutants, and partial functional redundancy has hampered the functional analysis in plants. Here, we report the identification of previously unrecognized embryonic lethal *Arabidopsis* mutants deficient in mitochondrial glutaredoxin S15 (GRXS15). Recombinant GRXS15 coordinates an iron-sulfur cluster in the presence of reduced glutathione as a cofactor. Genetic interference with glutathione binding through targeted mutagenesis diminished the ability of the protein to complement a yeast mutant lacking the homologous mitochondrial Grx5p. Similarly, mutated GRXS15 variants were not able to fully complement the lethal *Arabidopsis* mutants. Partial complementation resulting in a dwarf phenotype and severely diminished aconitase activity uncovered the role of mitochondrial GRXS15 in iron-sulfur protein maturation.

Author contributions: A.M., C.B., M.S., and A.J.M. designed research; A.M., I.A., T.N., J.P.-T., U.M., and N.R. performed research; C.B. and N.R. contributed new reagents/analytic tools; A.M., S.W., U.M., R.L., C.B., N.R., and A.J.M. analyzed data; A.M., C.B., N.R., M.S., and A.J.M. wrote the paper; and S.W. performed structural modeling.

The authors declare no conflict of interest.

This article is a PNAS Direct Submission.

Freely available online through the PNAS open access option.

[1]To whom correspondence should be addressed. Email: andreas.meyer@uni-bonn.de.

This article contains supporting information online at www.pnas.org/lookup/suppl/doi:10.1073/pnas.1510835112/-/DCSupplemental.

mitochondria (7) and *Arabidopsis* GRXS15 in the plastid stroma (10) or dual-targeted plastidic mitochondrial in bifunctional fluorescence complementation (BiFC) experiments with BolA4 (9). In proteome studies, GRXS15 has been repeatedly found in the mitochondria of *Arabidopsis* (11) and potato (12), but also in the chloroplast proteome of maize (13). The only phenotype of *grxs15*-null mutants described thus far is sensitivity toward H_2O_2, which led to the suggestion that GRXS15 may be involved in the maintenance of growth and development under oxidative stress conditions (10).

Here, we provide evidence that GRXS15 is an essential component of the mitochondrial ISC machinery that for a long time has been controversial because of the lack of suitable mutants and the failure to complement yeast cells lacking the orthologous gene. The results from in vitro ISC reconstitution and transfer assays and complementation of null mutants in yeast and *Arabidopsis* with mutated variants of GRXS15 demonstrate that GRXS15 coordinates an ISC and is likely essential for the delivery of ISC to apoproteins in mitochondria, serving in particular for the maturation of ISC into aconitase.

Results

Glutaredoxin GRXS15 Is Localized in Mitochondria. The *Arabidopsis* genome encodes 31 GRXs that cluster in three subgroups (Fig. S1). In this gene family, the monothiol GRXS15 could be the only member in mitochondria, but as explained above, its subcellular localization remains controversial. To resolve this uncertainty, the predicted 37-aa target peptide (TP_{GRXS15}; based on TargetP) and the full-length sequence of GRXS15 were cloned in frame with GFP under control of the 35S promoter and stably expressed in *Arabidopsis*. In both cases, the GFP signal was exclusively localized in mitochondria (Fig. 1*A*). This result was further corroborated through protein gel blot analysis in which GRXS15 was only detectable in isolated mitochondria but not in chloroplasts (Fig. 1*B*). In whole-leaf extracts of wild-type plants, no GRXS15 was detectable consistent with decreased relative abundance of mitochondrial proteins.

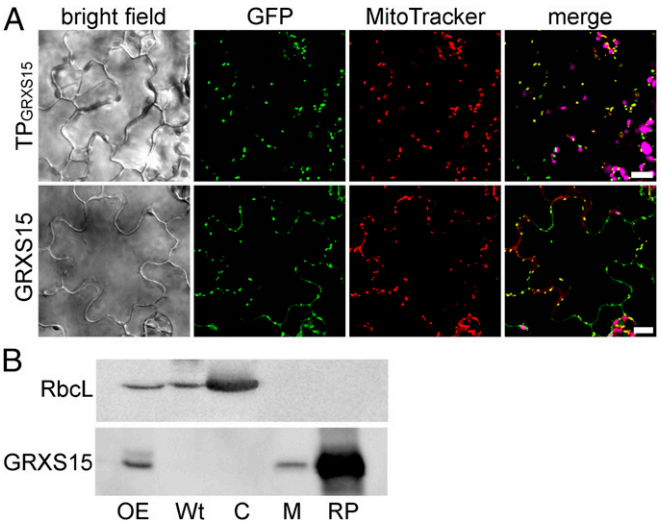

Fig. 1. Subcellular localization of GRXS15 in *Arabidopsis*. (*A*) Expression of $35S_{pro}$:TP_{GRXS15}:*GFP* and $35S_{pro}$:*GRXS15*:*GFP* in leaf epidermal cells. GFP, green; MitoTracker, red; chlorophyll autofluorescence, magenta. (Scale bars: 1 μm.) (*B*) Protein gel blot analysis with antiserum raised against *Arabidopsis* GRXS15. Fifteen micrograms of protein isolated from whole leaves of a GRXS15 overexpression plant (OE) and a wild-type plant (Wt) as well as proteins of isolated wild-type chloroplasts (C) and wild-type mitochondria (M) were loaded along with 0.5 μg of recombinant protein (RP). Immunoreactivity of the large subunit of RuBisCO (RbcL) served as control for purity of the mitochondrial preparation.

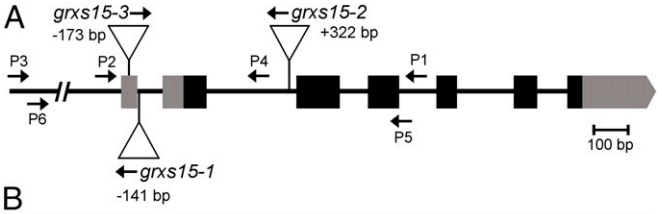

B

progeny genotype				
parental line	*GRXS15*/*GRXS15*	*GRXS15*/*grxs15*	*grxs15*/*grxs15*	χ^2- value
grxs15-2	23	49	0	0.06 (p = 0.97)
grxs15-3	18	38	0	0.04 (p = 0.98)
seed development				
parental line	aborted seeds	normal seeds		χ^2- value
grxs15-2	273	910		2.4 (p = 0.3)
grxs15-3	177	688		9.5 (p = 0.008)

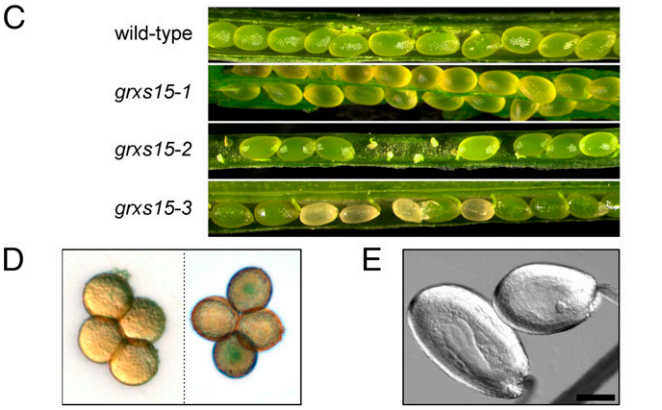

Fig. 2. Isolation and characterization of *grxs15* mutants. (*A*) Physical map of the *GRXS15* gene according to the gene model At3g15660.2. Introns are represented by lines and exons as boxes. Both UTRs are depicted in gray. The primers used for genotyping are indicated by numbered arrows. The T-DNA insertions of the mutant lines *grxs15-1*, *grxs15-2*, and *grxs15-3* are shown as inverted triangles with the identified insertion site relative to the start codon indicated. Nonnumbered arrows depict the left border (LB) primers used for genotyping and indicate the orientation of the T-DNA. (*B*) Segregation pattern and seed development of *grxs15* T-DNA insertion mutants. χ^2 values for the progeny genotype are calculated on an expected ratio of 1:2 and for seed development on an expected ratio of 3:1. The degree of freedom is in both cases 2. (*C*) Opened siliques from wild-type, *grxs15-1*, *grxs15-2*, and *grxs15-3* plants. (*D*) GUS labeling of *qrt* pollen tetrads from a segregated plant homozygous for the wild-type allele *GRXS15* (*Left*) or from a heterozygous *grxs15-2* plant (*Right*). (*E*) Differential interference contrast image of normal (*Left*) and transparent (*Right*) seed from the same silique of a *grxs15-3* plant. (Scale bar: 150 μm.)

Disruption of *GRXS15* Causes Early Embryo Abortion. To gain insight into the physiological role of GRXS15 in *Arabidopsis*, three T-DNA lines for the gene locus At3g15660 were isolated. These mutants included two lines with insertions in the 5′-UTR, denominated as *grxs15-1* and *grxs15-3* as well as a line with an insertion in the first intron of the coding sequence (*grxs15-2*; Fig. 2*A*). Left border flanking sequences of the T-DNA insertions in *grxs15-1*, *grxs15-3*, and *grxs15-2* were sequenced, and the insertion sites were mapped to positions −141, −173, and +322 bp relative to the start codon, respectively. Homozygous *grxs15-1* plants were phenotypically indistinguishable from wild type under normal growth conditions (Fig. 2*C* and Fig. S2). Whereas in wild-type plants the gene is transcribed into two different transcripts annotated as At3g15660.1 and At3g15660.2, *grxs15-1* contains only one transcript with a truncated 5′-UTR without obvious changes in transcript abundance (Fig. S2). Because this result implies that *grxs15-1* is not a null mutant, it was excluded from further analysis. In contrast, no homozygous *grxs15-2* and *grxs15*-3 mutants were found. In both cases,

selfed heterozygous plants segregated in a 1:2 (susceptible: resistant) pattern (Fig. 2*B*). The mutant *grxs15-2* was generated with a T-DNA containing a GUS gene driven by a pollen-specific promoter in the *quartet* (*qrt*) background that prevents separation of pollen after meiosis. Here, heterozygous plants always produced pollen tetrads with two GUS-positive pollen, which strongly suggests the absence of a second unlinked T-DNA insertion (Fig. 2*D*). Analysis of developing seeds from selfed *grxs15-2* and *grxs15-3* plants revealed frequent abortion (Fig. 2*C*). Whereas 23% of aborted *grxs15-2* seeds were still supporting the hypothesis of a 3:1 (viable:aborted) segregation, abortion in *grxs15-3* was slightly less frequent with approximately 20% (Fig. 2*B*). Interestingly, abortion in *grxs15*-2 occurred at an early stage after fertilization, whereas the presumed homozygous seeds in *grxs15-3* progressed significantly further in development and even initiated endosperm formation. The seeds nevertheless stayed transparent because embryo development was arrested at globular stage (Fig. 2*E*).

To further confirm that the observed embryo arrest was caused specifically by disruption of *GRXS15*, both null mutants were complemented with wild-type *GRXS15* driven by the UBQ10 promoter through transformation of the female gametophyte. All complemented plants were phenotypically normal, demonstrating the importance of GRXS15 for plant growth and development (Fig. S2*G*). The viable T_2 progeny of complemented *grxs15-2* plants all contain the *GRXS15* transgene (Fig. S2*H*), indicating that a loss of the complementation construct due to segregation causes lethality. These complementation data validate the conclusion that the embryo lethality is due to GRXS15 deficiency.

GRXS15 Partially Complements Δ*grx5* Yeast Cells. Because GRXS15 is the only confirmed GRX in *Arabidopsis* mitochondria and shares 33% amino acid identity with the yeast mitochondrial monothiol Grx5p (Fig. S3*A*), yeast Δ*grx5* strains displaying distinct growth defects were exploited for functional complementation studies. The original GRXS15 target peptide of 37 aa is sufficient for targeting GFP or a GRXS15-GFP fusion to mitochondria in yeast (Fig. 3*A*), as in plants. Therefore, the full-length sequence of *GRXS15* was used for detailed complementation studies. Multiple complementation experiments with different Δ*grx5* deletion strains consistently resulted in partial rescue of Δ*grx5* (Fig. 3*B* and Fig. S3*B*). Expression of GRXS15 also diminished the sensitivity of Δ*grx5* to the oxidative agent diamide but not the respiratory growth defect on glycerol (Fig. 3*B*). These observations strongly point at a partial functional conservation of GRXS15 between yeast and *Arabidopsis*.

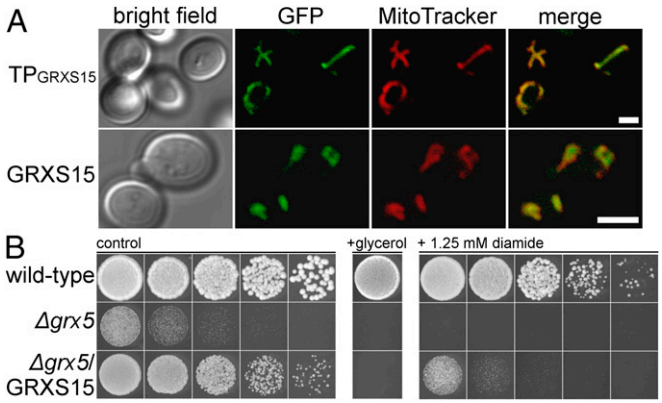

Fig. 3. Complementation of the yeast Δ*grx5* mutant by *Arabidopsis* GRXS15. (*A*) Subcellular localization of TP_{GRXS15}:GFP or GRXS15:GFP in *Saccharomyces cerevisiae* cells. Cultures were grown in liquid drop-out medium before incubation with the mitochondrial marker MitoTracker. GFP, green; MitoTracker, red. (Scale bars: 2 μm.) (*B*) Yeast growth on drop-out medium. Serial fivefold dilutions of wild type (BY4742) and the respective Δ*grx5* mutant (YPL059w), transformed with an empty vector, and the Δ*grx5* mutant transformed with GPD_{pro}:*GRXS15* were spotted on plates containing glucose (*Left*) or glucose with 1.25 mM diamide (*Right*) and grown at 30 °C. No growth was observed on drop-out medium containing glycerol instead of glucose to enforce respiratory growth (*Center*). One representative experiment from three independently performed experiments is shown.

Recombinant GRXS15 Lacks Oxidoreductase Activity but Binds an Iron-Sulfur Cluster. GRXS15 has been found among potential thioredoxin targets of plant mitochondria by affinity chromatography (14), suggesting that GRXS15 may act as an oxidoreductase, as proposed for yeast Grx5p (15). Thus, recombinant GRXS15 lacking the first 37 aa was analyzed for potential oxidoreductase activity. In the 2-hydroxyethyl disulfide (HED) assay, reductive activity of GRXS15 was only just above background and less than 3% of the activity observed for the *Arabidopsis* dithiol GRXC1 used as a reference (Fig. S4*A*). In an alternative assay with redox-sensitive GFP2 (roGFP2; ref. 16), no catalytic activity could be detected for the reduction of oxidized roGFP2 with reduced glutathione (GSH), whereas a residual catalytic effect was observed for the oxidation of roGFP2 with glutathione disulfide (GSSG). This effect, however, was approximately 30 times lower than catalysis by GRXC1 (Fig. S4 *C* and *D*). These results indicate that GRXS15 does not efficiently catalyze the formation or reduction of GSH-mixed disulfides.

To test the alternative hypothesis that GRXS15 is involved in supplying ISC to mitochondrial proteins, we first analyzed the capacity of a recombinant GRXS15 to bind an ISC. *Escherichia coli* cells expressing GRXS15 did not display the strong characteristic brownish color associated with the presence of an ISC in overexpressed proteins. However, when the recombinant protein was purified in the presence of 4 mM GSH, the UV-visible spectrum showed a pronounced shoulder at 420 nm, indicating that ISC coordination by GRXS15 occurred in *E. coli*. Because GRXS15 ISC incorporation was likely far from completion, we have performed in vitro reconstitution assays under anaerobic conditions by using the purified apoprotein. In this case, the visible part of the absorption spectrum of the reconstituted protein presented a prominent absorbance peak at approximately 420 nm compared with the apoprotein (Fig. 4*A*), which is characteristic for the presence of an $[2Fe\text{-}2S]^{2+}$ cluster or a mixture of $[2Fe\text{-}2S]^{2+}$ and linear $[3Fe\text{-}4S]^{+}$ clusters (17). Next, we evaluated the capacity of GRXS15 to transfer its ISC to an acceptor protein. Among mitochondrial Fe-S proteins, the mitochondrial ferredoxin 1 (MFDX1), which can bind an $[2Fe\text{-}2S]^{2+}$ cluster, was an obvious candidate. After purifying the recombinant protein and stripping the ISC by acidic precipitation, ISC transfer to the apoprotein was monitored over time by visualizing the newly formed holo-MFDX1 on native polyacrylamide gels (Fig. 4*C*). There was a clear gradual increase of holo-MFDX1. The initial transfer reaction was fast because at the 0 min timepoint, which was taken after mixing, spinning, and pipetting times, an appreciable amount of holo-MFDX1 had already formed. However, no further formation of holo-MFDX1 was observed after 45 min although some apo-MFDX1 was still available. The identity of the final product as MFDX1 containing the native $[2Fe\text{-}2S]^{2+}$ cofactor was confirmed by CD spectroscopy (Fig. 4*D*).

Diminished GSH Coordination by GRXS15 Limits the Ability To Complement Yeast Δ*grx5*. Based on the ability of GRXS15 to coordinate an ISC in vitro, we built a homology model with human GLRX5 as template (Fig. S5*A*). Monothiol GLRX5 coordinates an ISC, is mitochondria-resident and shares 37% identity with GRXS15. We then compared GRXS15 candidate residues for noncovalent binding of GSH as a prerequisite for ISC coordination to other GRX structures (Fig. 4*B*). Whereas position K_{83} is fully conserved in all analyzed GRX structures, positions K_{120} and D_{146} are more variable but usually retain residues that may participate in GSH binding through hydrogen bonding (Fig. S5 *B* and *C*).

The incorporation of an ISC led us to hypothesize that the ability of GRXS15 to complement the Δ*grx5* yeast mutant is based

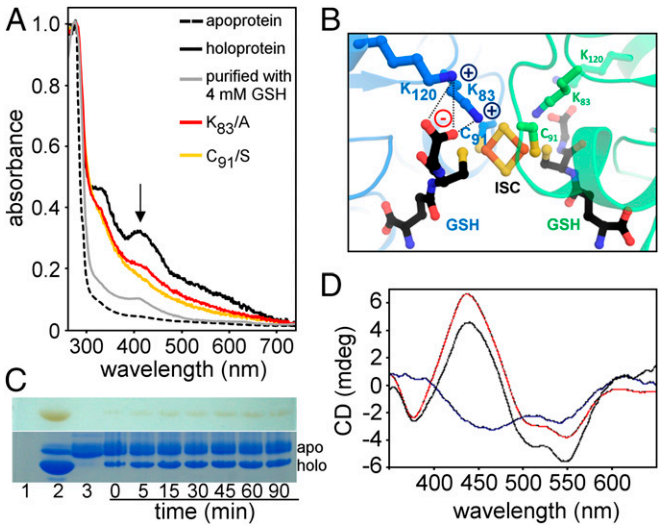

Fig. 4. Reconstitution of ISC in GRXS15 and ISC transfer to ferredoxin. (*A*) Reconstitution of an ISC in GRXS15. UV-visible spectra of apo- (dashed line) and holo-GRXS15 (straight black line), the K_{83}/A (red), and the C_{91}/S substituted protein (yellow) 2 h after reconstitution or directly after purification from *E. coli* in the presence of 4 mM GSH (gray). The spectra were normalized to the absorbance at 278 nm. (*B*) Structure modeling of GRXS15. A homology model was built by using Phyre2 with human mitochondrial GLRX5 as template. Highlighted are the amino acids K_{83} and K_{120} that may form hydrogen bonds with the carboxyl group of GSH as well as C_{91} that directly interacts with the ISC. (*C*) ISC transfer from holo-GRXS15 to apo-MFDX1. The transfer reaction was followed over a time-course of 90 min under anaerobic conditions by mixing holo-GRXS15 with apo-MFDX1 to a ~1.5:1 ratio in 200-μL reactions. Aliquots of 25 μL were removed at each time-point and separated on a native polyacrylamide gel. Lanes 1–3 correspond to approximately 20 μg of holo-GRXS15 (1), holo-MFDX1 (2), and apo-MFDX1 (3). *C, Upper* shows an unstained gel displaying the characteristic red-brownish color of holo-MFDX1. In *C, Lower*, a Coomassie blue-stained gel shows the relative proportions of apo- and holo-MFDX1. (*D*) CD spectrum comparison. Blue, initial CD spectrum of holo-GRXS15; black, CD spectrum after 60-min incubation of holo-GRXS15 and apo-MFDX1 at a ~1:1.5 ratio; red, reference CD spectrum for holo-MFDX1.

on its capacity to coordinate an ISC rather than on its reductase properties. Hence, GRXS15 was mutated to weaken GSH binding and, thus, interfere with ISC coordination. We reasoned that if ISC coordination is a critical function of GRXS15, less-efficient complementation should be expected as a result of the mutations. Based on the modeled structure, several substitutions were carried out to manipulate the direct environment of the putative ISC binding in a targeted manner. The mutations included charge inversions to gain drastic effects and substitutions by alanine that were anticipated to be less severe (Fig. S6*A*). Mutants lacking the active site cysteine (C_{91}) or carrying a K_{83}/E substitution were no longer able to complement the Δ*grx5* mutant, indicating the essential role of both amino acids (Fig. 5*A*). Substitution K_{83}/A turned out to be less severe and still allowed for residual complementation (Fig. 5*A*). Indeed, although the residual reducing activity was similar in the mutant variants compared with the native GRXS15, the K_{83}/A mutant was still able to coordinate an ISC, albeit less efficient than the wild type but better than the C_{91}/S mutant (Fig. S4*B* and Fig. 4*A*). Mutations of K_{120} generally had only diminutive effects on the ability of GRXS15 to complement Δ*grx5*. Mutagenesis of K_{124} and D_{146} had no influence on the ability to complement Δ*grx5* (Fig. S6 *B* and *C*).

To explore the functional impact of GRXS15 on cellular ISC homeostasis and maintenance of ISC proteins, yeast strains expressing the mutant variants in the Δ*grx5* background were analyzed for the activity of ISC-containing aconitase (ACO) as a marker. Whereas malate dehydrogenase (MDH), a mitochondrial non-ISC enzyme used as control, showed similar activity in all complemented lines and the wild type, ACO activity strongly depended on the mutations. Less severe mutations led to a minor proportional decrease in ACO/MDH activity ratio, whereas mutant variants that did not rescue Δ*grx5* growth showed low ACO activity (Fig. 5*B* and Fig. S7). The background activity may reflect a combination of residual mitochondrial ACO and cytosolic ACO. This result is in good correlation with the degree of growth rescue of Δ*grx5* expressing the different *Arabidopsis* GRXS15 variants.

To analyze whether the diminished function of GRXS15 has also an influence on the maturation of Fe-S proteins in the plant context, we complemented the *Arabidopsis grxs15-3* line with the mutated GRXS15 variants K_{120}/E and K_{83}/A based on the observation that both mutations lead to different degrees of partial complementation of the yeast Δ*grx5* mutant. In both cases, we could obtain homozygous plants. The *grxs15-3 UBQ10*$_{pro}$*:GRXS15* K_{120}/E plants showed no obvious differences in phenotype nor in ACO activity (Fig. S8 *A, B,* and *D*) despite differences in the expression level of GRXS15 (Fig. S8*C*). In contrast, *grxs15-3 UBQ10*$_{pro}$*:GRXS15* K_{83}/A plants showed severely reduced growth and reduced ACO activity (Fig. 6). Despite similar amounts of ACO protein detectable in leave extracts, ACO activity was decreased to a similar degree of approximately 35% residual activity in all complemented mutant plants (Fig. 6 *B* and *C*). This result may indicate that a low level of functional ACO in mitochondria is sufficient to maintain growth under nonstress conditions. The phenotypic differences between the complementation lines may be explained by GRXS15 transferring the ISC also to other apoproteins.

Discussion

In plant mitochondria, the redox balance is primarily maintained by ascorbate and glutathione acting together in the ascorbate–glutathione cycle (18). Although GSH is synthesized in plastids and in the cytosol, immunocytochemical staining suggested that mitochondria contain particularly high GSH concentrations (19). GRXs are generally considered to mediate reactions involving GSH as a cofactor for ISC coordination or for deglutathionylation/glutathionylation of target proteins (20). The yeast homolog of GRXS15, Grx5p, has been reported to act as a thiol reductase deglutathionylating substrate proteins (15). GRXS15 and the two plastidic GRXs, GRXS14 and GRXS16, are also capable of deglutathionylating the sulfur-transferase SUFE1 in vitro albeit at much lower rate than the plastidic type I GRXs, GRXC5 and GRXS12 (9). Our experiments from different GRX assays, however, suggest that GRXS15 has no reducing activity and, if at all, only a minor oxidation activity. A 20-fold lower activity observed for yeast Grx5p compared with

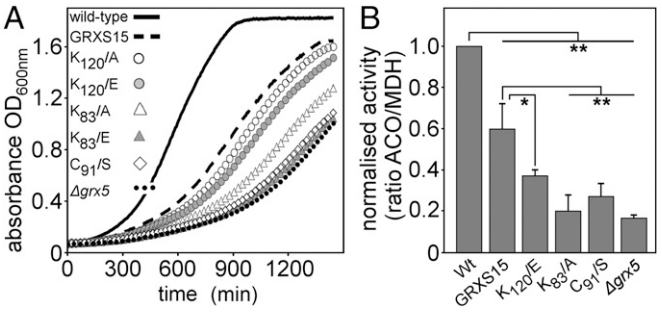

Fig. 5. Rescue of the yeast Δ*grx5* mutant defects by mutated GRXS15. (*A*) Growth of the yeast Δ*grx5* mutant, complemented with different versions of GRXS15. The absorbance at 600 nm was followed over time. One representative experiment from three independently performed experiments is shown. (*B*) Normalized ratio of aconitase (ACO)/malate dehydrogenase (MDH) activity. Enzyme activity was measured in total yeast cell extract of complemented Δ*grx5* mutant. Mean ± SEM ($n = 3$), Asterisks indicate statistically significant differences (Student *t* test: $*P \leq 0.1$; $**P \leq 0.05$) compared with wild type or GRXS15-complemented Δ*grx5* mutant.

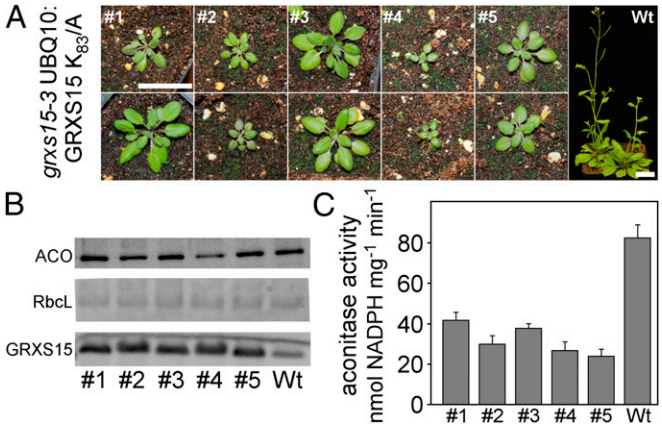

Fig. 6. Complementation of *grxs15-3* with *GRXS15* K_{83}*/A*. (*A*) Growth of 7-wk-old homozygous *grxs15-3 UBQ10*$_{pro}$*:GRXS15* K_{83}*/A* T_2 plants compared with the respective wild type. Shown are two plants per complemented line. (Scale bars: 2 cm.) (*B*) Protein expression of transgenic GRXS15 in *grxs15-3 UBQ10*$_{pro}$*: GRXS15* K_{83}*/A* plants compared with a nontransgenic wild type. In *Upper* aconitase and in *Lower* GRXS15 were detected by specific antibodies in total protein extract (15 μg of protein was loaded). In *Middle*, amido black staining of the membrane is shown focusing on the large subunit of RuBisCO (RbcL) as a control for protein loading. (*C*) Enzyme activity of aconitase in the *grxs15-3 UBQ10*$_{pro}$*:GRXS15* K_{83}*/A* plants compared with wild type ($n = 3 \pm$ SEM).

dithiol Grx1 with GSH as electron donor has been explained by inefficient reduction of monothiol GRXs by GSH (15). This result is in line with independent observations showing low or even negligible levels of thiol-disulfide oxidoreductase activity of several monothiol GRXs (21), suggesting that this function became secondary during evolution. However, GRXS17, a cytosolic multidomain GRX, is able to reduce the glutathionylated and the homodimeric form of BolA2, suggesting that the in vivo activity of BolA proteins could be modulated in a redox-dependent manner (9). For GRXS15, an interaction with the BolA domain of SufE1 has been shown by Y2H. This result, however, remains inconclusive because SufE1-YFP was reported to be dual-targeted to plastids and mitochondria when expressed heterologously in tobacco leaves (22) but so far has never been reported in proteome analyses from *Arabidopsis* mitochondria. Indeed no such interaction was found in BiFC assays in *Arabidopsis* protoplasts (9). In contrast, interaction of GRXS15 with the dual-targeted BolA4 was found in Y2H and BiFC assays in both mitochondria and chloroplasts (9). In this case, the plastidic interaction might be due to the overexpression of GRXS15, which is routed to chloroplasts via the BolA4 interaction. Little is known about BolAs in plants, but in human cells, the mitochondrial BOLA3 has been suggested to interact with GLRX5 in the maturation of lipoate-containing 2-oxoacid dehydrogenases and assembly of respiratory chain complexes (23). Regarding 2-oxoacid dehydrogenases, lipoic acid synthase (LIAS) catalyzes the lipoylation of the octanoylated apoproteins. LIAS contains a Fe_4S_4 cluster, suggesting that a BOLA3/GLRX5 heterodimer is required for its maturation. Given that *Arabidopsis* contains also a mitochondrial-targeted lipoic acid synthase (At2g20860), a similar function for GRXS15 appears conceivable.

Among poplar monothiol GRXs, the two plastidic isoforms, GRXS14 and GRXS16, complement the yeast Δ*grx5* mutant, whereas poplar GRXS15 was shown to be relatively inefficient and there was no indication that it could incorporate an ISC (7). Triggered by the identification of embryonic lethal *Arabidopsis grxs15* null mutants and the assumption that GRXS15 is the only mitochondrial GRX, we investigated the ability of *Arabidopsis* GRXS15 to complement yeast Δ*grx5* mutants. With this isoform, complementation of different Δ*grx5* yeast strains worked, although we never achieved a 100% complementation. Interestingly, the increase of the ACO/MDH activity for GRXS15 complemented Δ*grx5* (~0.59) compared with the empty vector control (~0.17) was higher than the normalized ratio for Δ*grx5* complemented with poplar GRXS15 (~0.26; ref. 7). The reason for only partial complementation is unknown, but one can speculate about differences between yeast and *Arabidopsis* proteins leading to less stable ISC coordination or partially impaired protein–protein interactions as a result of the coevolution between the interacting proteins within a given organism. For instance, compared with yeast Grx5p, plant GRXS15 isoforms have a clear N-terminal extension containing many conserved Asp residues, whereas they have a slightly shorter C-terminal part missing charged residues found in Grx5p. Considering that the C-terminal part of monothiol GRXs was shown to be responsible for protein–protein interaction (24), variations in this protein region might be crucial. Another important difference is that yeast Grx5p contains an additional cysteine residue (C_{90} or C_{117} including the targeting sequence) implicated in intramolecular disulfide exchange reactions (15). Whereas genetic analyses indicated that this cysteine does not seem essential for ISC biogenesis (25), Zhang et al. showed in mutational studies that this cysteine is required for the assembly of Fe_4S_4 cluster and that the Fe_4S_4 cluster-bound form of Grx5p is competent for restoring the activity of recombinant ACO in vitro (17). Although this cysteine is present in most algal isoforms, it is replaced by a serine in orthologs from terrestrial plants, except *Selaginella moellendorffii* (26). The ability to complement the Δ*grx5* mutant likely implies that GRXS15 is involved in ISC biosynthesis or transfer in *Arabidopsis* mitochondria. Reconstitution assays confirmed the incorporation of an ISC and the resulting A_{420}/A_{280} ratio of 0.36 was in a similar range as for other monothiol GRXs coordinating ISCs [GRXS14: 0.31 ± 0.04 (7) and GRXS17: 0.29 (8)]. The ability to coordinate ISCs and the ability to transfer the ISC to MFDX1 in vitro shown here as well as the interaction with the transfer protein ISA (27) all point to a role of GRXS15 in ISC transfer similar to yeast Grx5p. This interpretation is strongly supported by the fact that mutations in GRXS15 interfering with the binding of the GSH cofactor required for ISC coordination impair the ability to complement the Δ*grx5* yeast mutant. Because the role of GRXS15 seems restricted to ISC maturation, future work needs to explain how the interaction that has been shown to occur efficiently between the glutathione pool and thiol proteins is mediated (28, 29).

In contrast to Δ*grx5* yeast cells, loss of GRXS15 in *Arabidopsis* causes embryonic lethality. Viability of Δ*grx5* is maintained by the mitochondrial dithiol Grx2p as a backup, and Δ*grx2*Δ*grx5* mutants are synthetic lethal (30). In zebrafish, where Grx2 seems to be mainly localized in the cytosol, deficiency of Grx5 is lethal between 7 and 10 d after fertilization (6, 31). Taken together, the data presented in this paper conclusively show that GRXS15 is essential in plant mitochondria. Furthermore, the knockout of other genes that are essential in the mitochondrial ISC machinery like frataxin or IBA57 results in an embryo-lethal phenotype (32, 33). Despite the necessity of GRXS15 during the vegetative phase, the segregation patterns indicate that GRXS15 is less critical during fertilization. This phenomenon may be explained by residual ISC assembled before meiosis or by the fact that energy metabolism in pollen tubes can undergo fast rearrangements shifting from aerobic respiration to ethanol fermentation (34). Pollen tube growth has been shown to continue even under anaerobic conditions or on inhibitors of the respiratory electron transport or ATP synthase albeit at lower speed (34, 35). This effect may explain the slight deviations from Mendelian segregation observed for selfed *grxs15-3* mutants.

In summary, this work expands the role of GRXs in the biogenesis of Fe-S proteins by identifying GRXS15 as an essential component of the mitochondrial ISC assembly machinery in *Arabidopsis*. The isolation of null mutants and their characterization as being embryonic lethal solves a long-standing mystery about the role of GRXS15.

Materials and Methods

See *SI Materials and Methods* and Tables S1 and S2 for biological materials, growth conditions, genetic analysis, and cloning details.

Microscopy. Subcellular localization of GRXS15 was observed after GFP tagging by confocal microscopy on a Zeiss LSM780 with instruments settings detailed in *SI Materials and Methods*.

Protein Purification. Recombinant proteins were expressed and purified as described (16). Purification of GRXS15 was performed under aerobic conditions with or without 4 mM GSH. The protein content was quantified by the Bradford assay with BSA as standard. For all other proteins, details are described in *SI Materials and Methods*.

ISC Reconstitution and Transfer. The ISC reconstitution assay was performed as described (36). UV-VIS spectra were recorded by using a plate reader (CLARIOstar; BMG). Transfer of ISC from GRXS15 to MFDX1 was followed by native PAGE and CD spectrometry. Full details are described in *SI Materials and Methods*.

Enzyme Assays. All assays were carried out at 25 °C on a plate reader (POLARstar Omega; BMG). Interaction of roGFP2 with GRXS15 or GRXC1 from *Arabidopsis* was performed as described (37) by using 1 μM roGFP2 as well as 3 μM GRXS15 or GRXC1. For all other assays, details are described in *SI Materials and Methods*.

ACKNOWLEDGMENTS. We thank Dr. Ninghui Cheng for providing *grxs15-2* seeds and Dr. Enrique Herrero for yeast strains with defects in Grx5p. Financial support by the Deutsche Forschungsgemeinschaft (DFG) Grant ME1567/5-1 (to A.J.M.) and within the priority program Dynamics of thiol-based redox switches in cellular physiology (DFG SPP1710) Grants ME1567/9-1 (to A.J.M.) and BE3259/5-1 (to C.B.) and Emmy Noether Program Grant SCHW1719/1-1 (to M.S.) is gratefully acknowledged. The scientific activities of the Bioeconomy Science Center were financially supported by the Ministry of Innovation, Science and Research within the framework of the NRW Strategieprojekt BioSC No. 313/323-400-002 13.

1. Schaedler TA, et al. (2014) A conserved mitochondrial ATP-binding cassette transporter exports glutathione polysulfide for cytosolic metal cofactor assembly. *J Biol Chem* 289(34):23264–23274.
2. Boyd ES, Thomas KM, Dai Y, Boyd JM, Outten FW (2014) Interplay between oxygen and Fe-S cluster biogenesis: Insights from the Suf pathway. *Biochemistry* 53(37):5834–5847.
3. Couturier J, Touraine B, Briat JF, Gaymard F, Rouhier N (2013) The iron-sulfur cluster assembly machineries in plants: Current knowledge and open questions. *Front Plant Sci* 4:259.
4. Picciocchi A, Saguez C, Boussac A, Cassier-Chauvat C, Chauvat F (2007) CGFS-type monothiol glutaredoxins from the cyanobacterium Synechocystis PCC6803 and other evolutionary distant model organisms possess a glutathione-ligated [2Fe-2S] cluster. *Biochemistry* 46(51):15018–15026.
5. Rodríguez-Manzaneque MT, Tamarit J, Bellí G, Ros J, Herrero E (2002) Grx5 is a mitochondrial glutaredoxin required for the activity of iron/sulfur enzymes. *Mol Biol Cell* 13(4):1109–1121.
6. Wingert RA, et al.; Tübingen 2000 Screen Consortium (2005) Deficiency of glutaredoxin 5 reveals Fe-S clusters are required for vertebrate haem synthesis. *Nature* 436(7053):1035–1039.
7. Bandyopadhyay S, et al. (2008) Chloroplast monothiol glutaredoxins as scaffold proteins for the assembly and delivery of [2Fe-2S] clusters. *EMBO J* 27(7):1122–1133.
8. Knuesting J, et al. (2015) Arabidopsis glutaredoxin S17 and its partner, the nuclear factor Y subunit C11/negative cofactor 2α, contribute to maintenance of the shoot apical meristem under long-day photoperiod. *Plant Physiol* 167(4):1643–1658.
9. Couturier J, et al. (2014) Monothiol glutaredoxin-BolA interactions: Redox control of Arabidopsis thaliana BolA2 and SufE1. *Mol Plant* 7(1):187–205.
10. Cheng NH (2008) AtGRX4, an Arabidopsis chloroplastic monothiol glutaredoxin, is able to suppress yeast grx5 mutant phenotypes and respond to oxidative stress. *FEBS Lett* 582(6):848–854.
11. Klodmann J, Senkler M, Rode C, Braun H-P (2011) Defining the protein complex proteome of plant mitochondria. *Plant Physiol* 157(2):587–598.
12. Salvato F, et al. (2014) The potato tuber mitochondrial proteome. *Plant Physiol* 164(2):637–653.
13. Huang M, et al. (2013) Construction of plastid reference proteomes for maize and Arabidopsis and evaluation of their orthologous relationships; the concept of orthoproteomics. *J Proteome Res* 12(1):491–504.
14. Balmer Y, et al. (2004) Thioredoxin links redox to the regulation of fundamental processes of plant mitochondria. *Proc Natl Acad Sci USA* 101(8):2642–2647.
15. Tamarit J, Belli G, Cabiscol E, Herrero E, Ros J (2003) Biochemical characterization of yeast mitochondrial Grx5 monothiol glutaredoxin. *J Biol Chem* 278(28):25745–25751.
16. Meyer AJ, et al. (2007) Redox-sensitive GFP in Arabidopsis thaliana is a quantitative biosensor for the redox potential of the cellular glutathione redox buffer. *Plant J* 52(5):973–986.
17. Zhang B, et al. (2013) Monothiol glutaredoxins can bind linear $[Fe_3S_4]^+$ and $[Fe_4S_4]^{2+}$ clusters in addition to $[Fe_2S_2]^{2+}$ clusters: Spectroscopic characterization and functional implications. *J Am Chem Soc* 135(40):15153–15164.
18. Chew O, Whelan J, Millar AH (2003) Molecular definition of the ascorbate-glutathione cycle in Arabidopsis mitochondria reveals dual targeting of antioxidant defenses in plants. *J Biol Chem* 278(47):46869–46877.
19. Zechmann B, Mauch F, Sticher L, Müller M (2008) Subcellular immunocytochemical analysis detects the highest concentrations of glutathione in mitochondria and not in plastids. *J Exp Bot* 59(14):4017–4027.
20. Rouhier N, Lemaire SD, Jacquot J-P (2008) The role of glutathione in photosynthetic organisms: Emerging functions for glutaredoxins and glutathionylation. *Annu Rev Plant Biol* 59(1):143–166.
21. Fernandes AP, et al. (2005) A novel monothiol glutaredoxin (Grx4) from Escherichia coli can serve as a substrate for thioredoxin reductase. *J Biol Chem* 280(26):24544–24552.
22. Xu XM, Møller SG (2006) AtSufE is an essential activator of plastidic and mitochondrial desulfurases in Arabidopsis. *EMBO J* 25(4):900–909.
23. Cameron JM, et al. (2011) Mutations in iron-sulfur cluster scaffold genes NFU1 and BOLA3 cause a fatal deficiency of multiple respiratory chain and 2-oxoacid dehydrogenase enzymes. *Am J Hum Genet* 89(4):486–495.
24. Roret T, et al. (2014) Structural and spectroscopic insights into BolA-glutaredoxin complexes. *J Biol Chem* 289(35):24588–24598.
25. Bellí G, et al. (2002) Structure-function analysis of yeast Grx5 monothiol glutaredoxin defines essential amino acids for the function of the protein. *J Biol Chem* 277(40):37590–37596.
26. Couturier J, Jacquot JP, Rouhier N (2009) Evolution and diversity of glutaredoxins in photosynthetic organisms. *Cell Mol Life Sci* 66(15):2539–2557.
27. Arabidopsis Interactome Mapping Consortium (2011) Evidence for network evolution in an Arabidopsis interactome map. *Science* 333(6042):601–607.
28. Palmieri MC, Lindermayr C, Bauwe H, Steinhauser C, Durner J (2010) Regulation of plant glycine decarboxylase by s-nitrosylation and glutathionylation. *Plant Physiol* 152(3):1514–1528.
29. Schwarzländer M, Fricker MD, Sweetlove LJ (2009) Monitoring the in vivo redox state of plant mitochondria: Effect of respiratory inhibitors, abiotic stress and assessment of recovery from oxidative challenge. *Biochim Biophys Acta* 1787(5):468–475.
30. Rodríguez-Manzaneque MT, Ros J, Cabiscol E, Sorribas A, Herrero E (1999) Grx5 glutaredoxin plays a central role in protection against protein oxidative damage in Saccharomyces cerevisiae. *Mol Cell Biol* 19(12):8180–8190.
31. Bräutigam L, et al. (2011) Vertebrate-specific glutaredoxin is essential for brain development. *Proc Natl Acad Sci USA* 108(51):20532–20537.
32. Busi MV, et al. (2006) Deficiency of Arabidopsis thaliana frataxin alters activity of mitochondrial Fe-S proteins and induces oxidative stress. *Plant J* 48(6):873–882.
33. Waller JC, et al. (2012) Mitochondrial and plastidial COG0354 proteins have folate-dependent functions in iron-sulphur cluster metabolism. *J Exp Bot* 63(1):403–411.
34. Obermeyer G, Fragner L, Lang V, Weckwerth W (2013) Dynamic adaption of metabolic pathways during germination and growth of lily pollen tubes after inhibition of the electron transport chain. *Plant Physiol* 162(4):1822–1833.
35. Rounds CM, Hepler PK, Fuller SJ, Winship LJ (2010) Oscillatory growth in lily pollen tubes does not require aerobic energy metabolism. *Plant Physiol* 152(2):736–746.
36. Berndt C, et al. (2007) How does iron-sulfur cluster coordination regulate the activity of human glutaredoxin 2? *Antioxid Redox Signal* 9(1):151–157.
37. Aller I, Rouhier N, Meyer AJ (2013) Development of roGFP2-derived redox probes for measurement of the glutathione redox potential in the cytosol of severely glutathione-deficient rml1 seedlings. *Front Plant Sci* 4:506.
38. Edwards K, Johnstone C, Thompson C (1991) A simple and rapid method for the preparation of plant genomic DNA for PCR analysis. *Nucleic Acids Res* 19(6):1349.
39. Clough SJ, Bent AF (1998) Floral dip: A simplified method for *Agrobacterium*-mediated transformation of Arabidopsis thaliana. *Plant J* 16(6):735–743.
40. Brach T, et al. (2009) Non-invasive topology analysis of membrane proteins in the secretory pathway. *Plant J* 57(3):534–541.
41. Karimi M, Inzé D, Depicker A (2002) GATEWAY vectors for Agrobacterium-mediated plant transformation. *Trends Plant Sci* 7(5):193–195.
42. Curtis MD, Grossniklaus U (2003) A gateway cloning vector set for high-throughput functional analysis of genes in planta. *Plant Physiol* 133(2):462–469.
43. Escobar MA, Geisler DA, Rasmusson AG (2006) Reorganization of the alternative pathways of the Arabidopsis respiratory chain by nitrogen supply: Opposing effects of ammonium and nitrate. *Plant J* 45(5):775–788.
44. Martínez-García JF, Monte E, Quail PH (1999) A simple, rapid and quantitative method for preparing Arabidopsis protein extracts for immunoblot analysis. *Plant J* 20(2):251–257.
45. Meyer J, Moulis J-M, Lutz M (1986) High-yield chemical assembly of [2Fe-2X] (X = S, Se) clusters into spinach apoferredoxin: Product characterization by resonance Raman spectroscopy. *Biochim Biophys Acta* 871(3):243–249.
46. Stehling O, et al. (2007) Investigation of iron-sulfur protein maturation in eukaryotes. Mitochondria, *Methods in Molecular Biology*, eds Leister D, Herrmann J (Humana Press, New York), Vol 372, pp 325–342.
47. Gietz RD, Schiestl RH (2007) High-efficiency yeast transformation using the LiAc/SS carrier DNA/PEG method. *Nat Protoc* 2(1):31–34.